Materials Letters 81 (2012) 41–44

Contents lists available at SciVerse ScienceDirect

Materials Letters

journal homepage: www.elsevier.com/locate/matlet

A change in morphology from anatase-TiO_2 nanoparticles to anatase-TiO_2 nanoflakes via electrospray

HyeLan An, Hyo-Jin Ahn *

Department of Materials Science and Engineering, Seoul National University of Science and Technology, Seoul 139-743, Republic of Korea

ARTICLE INFO

Article history:
Received 16 February 2012
Accepted 26 April 2012
Available online 3 May 2012

Keywords:
Anatase-TiO_2
Nanoparticles
Nanoflakes
Electrospray
Morphology

ABSTRACT

The change in morphology from anatase-TiO_2 nanoparticles to anatase-TiO_2 nanoflakes was induced using an electrospray method. The morphological, structural, and chemical properties of all samples were investigated using field-emission scanning electron microscopy (FESEM), transmission electron microscopy (TEM), X-ray diffraction (XRD), and X-ray photoelectron spectroscopy (XPS). To control their morphologies, the relative humidity in a closed electrospray chamber was maintained at 35% ± 3%, 55% ± 3%, and 75% ± 3%. The different morphologies during the transformation from anatase-TiO_2 nanoparticles to anatase-TiO_2 nanoflakes were a result of the different relative humidities in the closed electrospray chamber. As a result, anatase-TiO_2 nanoflakes were formed owing to the higher partial pressure of water in the atmosphere of the closed chamber and the slower solidification process of the charged jet.

1. Introduction

Nano-sized materials are currently of considerable interest owing to their unique optical, electrical, physical, chemical, and electrochemical properties when compared to those of bulk materials [1]. Nano-sized titanium oxide (TiO_2) has recently been receiving a great deal of attention because it is a very attractive material to academia and industry for use as pigments, solar cells, catalyst supports, etc. [2]. Therefore, for use in these various applications, a considerable amount of effort has been made to fabricate uniform nano-sized TiO_2 with morphology modification, for example, nanoparticles, nanosheets, nanowires, and nanotubes [2–5]. Various synthetic methods such as hydrolysis, hydrothermal, solvothermal, and electrospray techniques have been developed till date for the production of zero-dimensional nanostructures [2,3,6–8]. Among these methods, the electrospray technique is a simple, versatile, and cost-effective technology that can be used in a variety of fields for the fabrication of semi-conductive ceramics, polymer coating, protein films, and micro-pattering [9,10]. In the electrospray technique, a jet of liquid is sprayed toward a collector under a strong electric field. Three major variables influence the synthesis of materials by the electrospray method: (I) solution conditions such as the solvents and precursors used, (II) processing conditions such as voltages and feeding rates, and (III) ambient conditions such as temperature and humidity. However, studies conducted to date have focused on TiO_2 nanoparticles or nanospheres. For examples, Modesto-Lopez et al. synthesized TiO_2 agglomerates via electrospray and demonstrated differences in their morphology, thickness, and porosity [7]. Hwang et al. reported the fabrication of hierarchically-structured mesoporous TiO_2 nanospheres prepared with electrospray for use in dye-sensitized solar cells [8]. However, despite the many important applications of nano-sized TiO_2, the relationship between variations in morphology and ambient conditions (relative humidity) during the electrospray process has not yet been investigated. Therefore, in this study, the morphological change from anatase-TiO_2 nanoparticles to anatase-TiO_2 nanoflakes by changing the relative humidity from 35% ± 3% to 75% ± 3% is demonstrated. In addition, the mechanism through which this change occurs is shown based on structural characteristics and chemical bonding states.

2. Experiments

Anatase-TiO_2 nanoparticles and nanoflakes were fabricated via electrospray. Titanium isopropoxide (97%, Aldrich) and acetic acid (99.7%, Aldrich) were dissolved in ethanol as a precursor and dispersant. The concentration of a Ti precursor in solvent for electrospray was fixed to ~3.1 wt.%. The precursor solution was stirred for 0.5 h at room temperature and the as-prepared solution was loaded into a syringe equipped with a 32-gauge stainless needle. The feeding rate of the solution was fixed at 0.02 ml/h by a syringe pump. The distance between the tip of the needle and collector was controlled at ~10 cm. A humidifier (WINIA, AWX-70PTB) inside a closed chamber was used to systematically control the relative humidity and the value of the relative humidity was monitored as a hygrometer. To control the morphological change from nanoparticles to nanoflakes, the humidity inside a closed chamber was maintained

* Corresponding author. Tel.: +82 2 970 6622; fax: +82 2 973 6657.
E-mail address: hjahn@seoultech.ac.kr (H-J. Ahn).

0167-577X/$ – see front matter © 2012 Elsevier B.V. All rights reserved.
doi:10.1016/j.matlet.2012.04.143

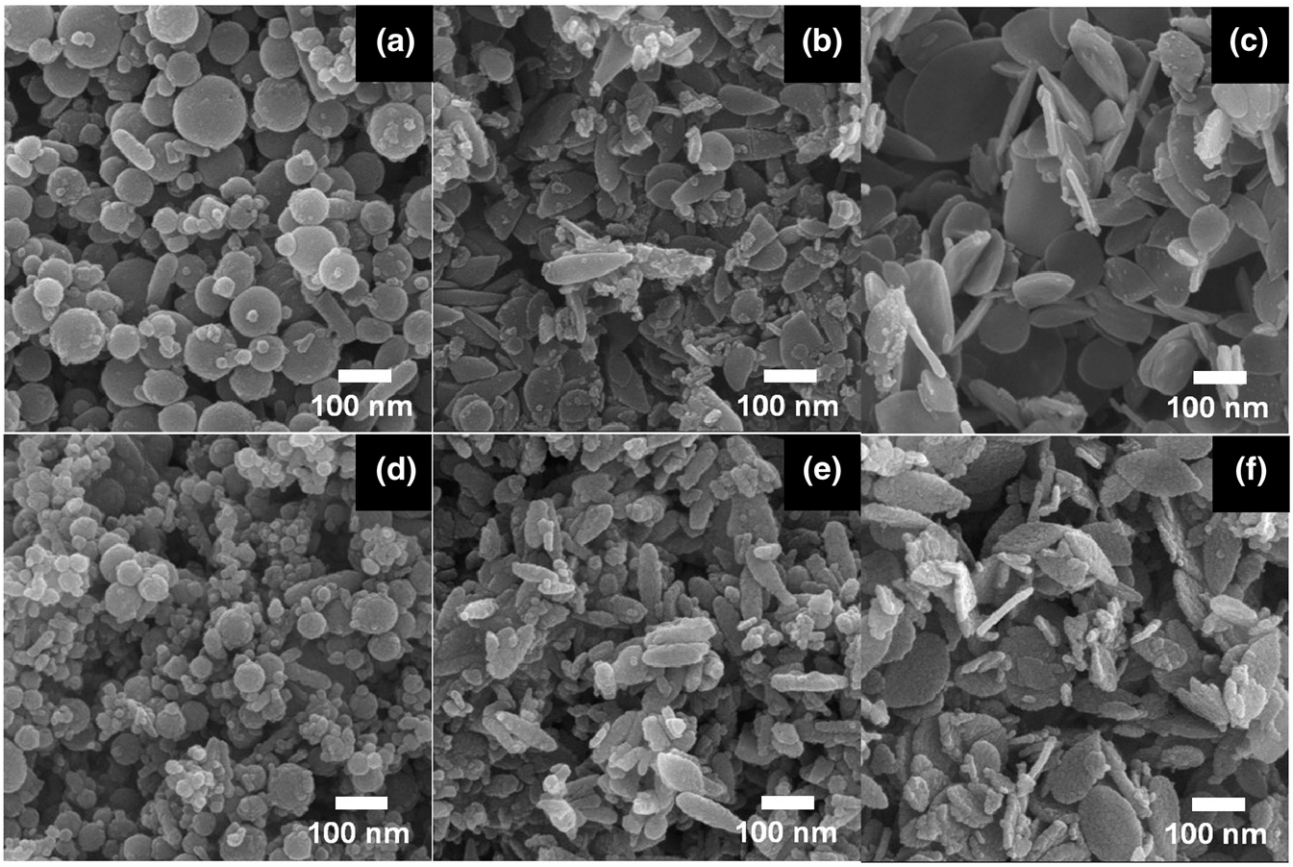

Fig. 1. FESEM images of samples A, B, and C before and after calcinations, (a)–(c) and (d)–(f), respectively.

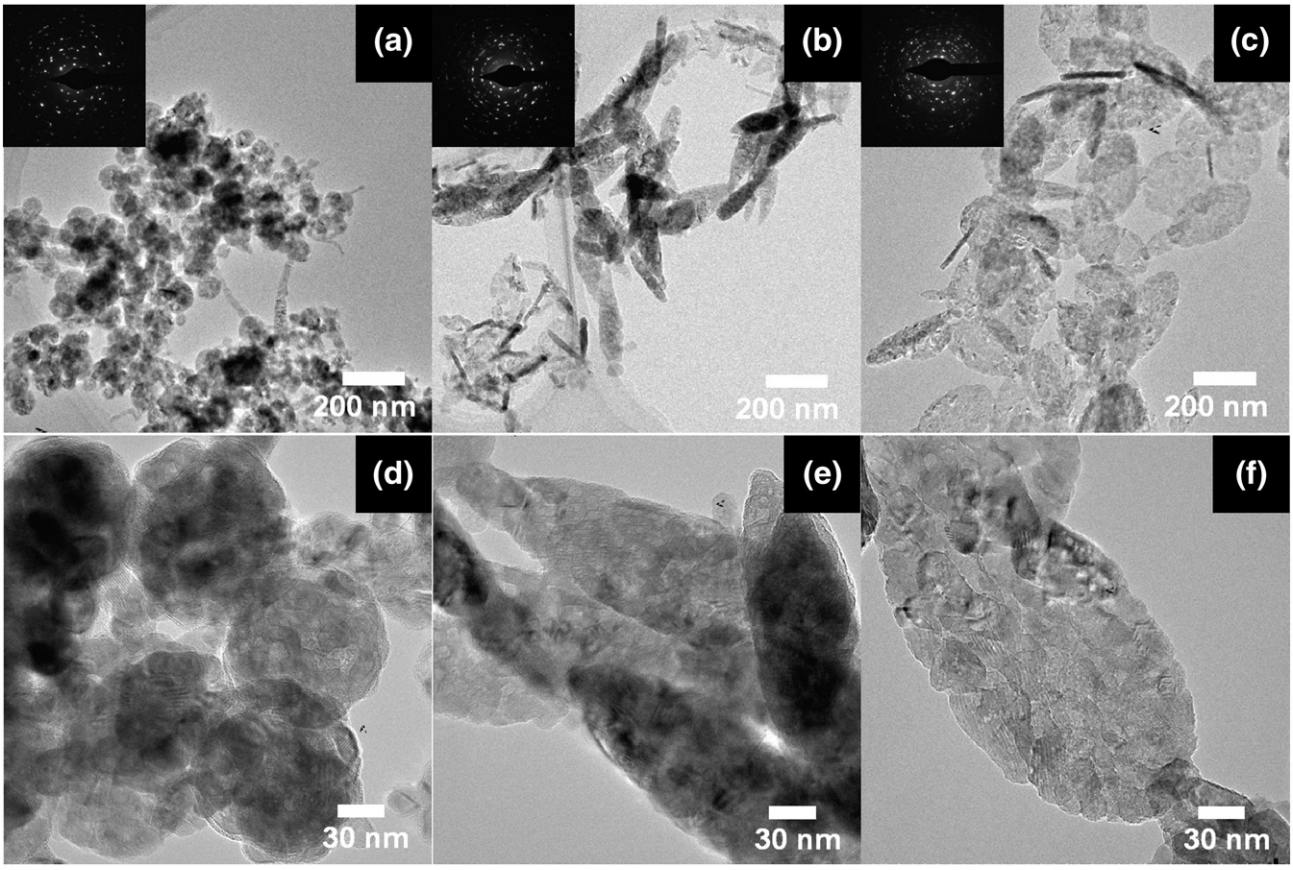

Fig. 2. TEM images and EDP patterns (panels (a)–(c)) of samples A, B, and C and enlarged TEM images (panels (d)–(f)) obtained from Fig. 2(a)–(c).

at 35 ± 3%, 55 ± 3%, and 75 ± 3% during the electrospray process to give samples A, B, and C, respectively. The voltage was maintained at 20 kV for sample A, 23 kV for sample B, and 23.5 kV for sample C by a power supply connected to the needle tip. The resulting samples were calcined at 500 °C for 5 h in air to allow crystallization. This process led to the successful fabrication of anatase-TiO_2 nanoparticles, anatase-TiO_2 semi-nanoflakes, and anatase-TiO_2 nanoflakes. To confirm the formation mechanism, the morphologies of the samples were examined using field-emission scanning electron microscopy (FESEM; Hitachi S-4700) and transmission electron microscopy (TEM; JEOL-2100 F, KBSI Suncheon center). The structural properties and chemical bonding states of the samples were investigated using X-ray diffraction (XRD; Rigaku Rint 2500) and X-ray photoelectron spectroscopy (XPS; ESCALAB 250).

3. Results and discussion

Fig. 1(a)–(c) and (d)–(f) show the FESEM images obtained from samples A, B, and C before and after the calcinations. Samples A, B, and C formed TiO_2 nanoparticles, TiO_2 semi-nanoflakes, and TiO_2 nanoflakes before calcination with diameters of ~20 to ~130 nm, ~30 to ~160 nm, and ~60 to ~190 nm, respectively (Fig. 1(a)–(c)). Interestingly, sample C produced a larger diameter owing to the formation of nanoflakes. Indeed, the thickness of sample C ranged from ~12 to ~18 nm. Taken together, these findings indicate that we successfully synthesized TiO_2 nanoflakes. Based on the overall experiment, we believed that the formation of nanoflakes was directly related to the relative humidity as a result of the higher partial pressure of water in the atmosphere of the closed chamber [11]. When a jet solution was sprayed on the collector, TiO_2 nanoparticles were flattened, resulting in a higher partial pressure of water. As a result, the TiO_2 nanoparticles changed to TiO_2 nanoflakes when there was a higher relative humidity (75% ± 3%) in the closed chamber.

The diameter of the samples after calcination at 500 °C ranged from ~15 to ~100 nm for sample A, ~20 to ~140 nm for sample B, and ~40 to ~160 nm for sample C. The diameters of all the samples were reduced by ~20% to 30% after calcination. However, the morphologies of the samples were unchanged in response to calcination.

Fig. 2(a)–(c) show the TEM images and electron diffraction patterns (EDP) obtained from samples A, B, and C after calcination at 500 °C. As shown in Fig. 2(a)–(c), the TEM images of samples A and B were observed as relatively dark regions owing to the greater thickness of the TiO_2 samples. In contrast, sample C was found to have relatively bright regions owing to the thinner thickness of the TiO_2 samples. It is well known that TEM is a microscopy technique in which electrons are passed through the samples. As the thickness increases, the beam of electrons has greater difficulty passing through the TiO_2 samples. As shown in Fig. 2(c), sample C had a uniform bright contrast, implying the successful formation of TiO_2 nanoflakes via electrospray. EDP (the top left) consists of diffuse ring patterns containing spots around the (000) spot, which is indicative of polycrystalline properties. To confirm the morphology of the TiO_2 samples, the TEM images were enlarged (Fig. 2(d)–(f)). TiO_2 nanoparticles, semi-nanoflakes, and nanoflakes consisting of small grains could be clearly observed. Taken together, the FESEM and TEM results demonstrate that the morphology changed from nanoparticles to nanoflakes.

To investigate the crystal structures of the samples, XRD was conducted after calcination. As shown in Fig. 3, XRD revealed that the samples produced characteristic peaks at 25.3°, 37.8°, 48.0°, 53.9°, and 55.1°, corresponding to the (101), (004), (200), (105), and (211) planes of the body-centered tetragonal structure of TiO_2 (space group $I4_1/amd$ [141]), respectively (JCPDS card No. 84-1286). These results indicate that all samples formed anatase structures.

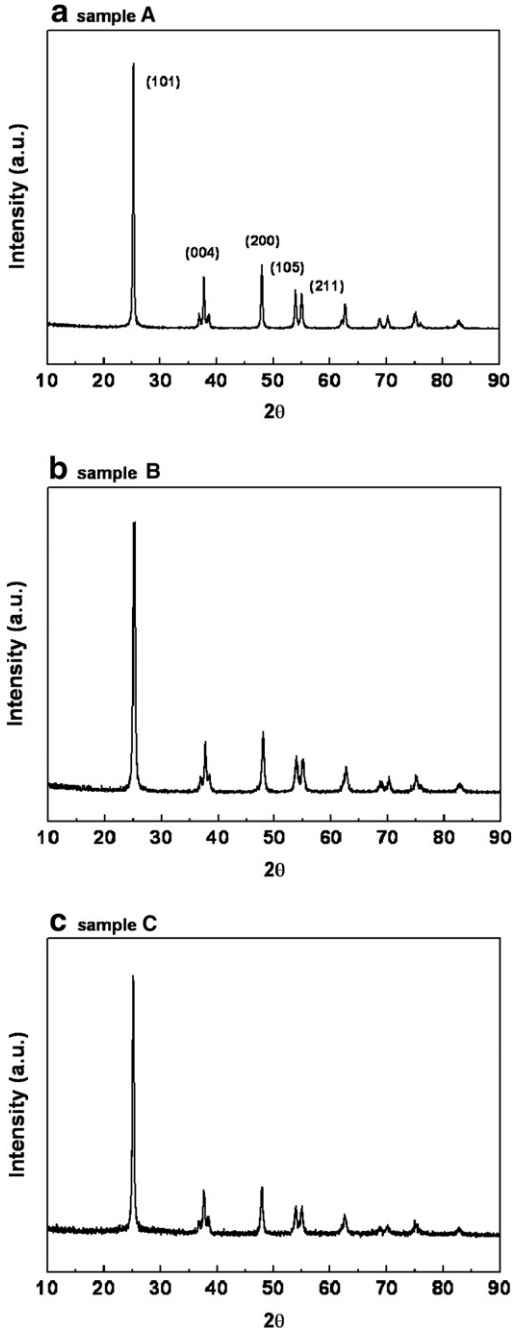

Fig. 3. XRD plots of samples A, B, and C obtained after calcination.

Fig. 4 shows the XPS spectra of the Ti 2*p* core level of samples A, B, and C. The XPS core-level spectra for Ti $2p_{3/2}$ and $2p_{1/2}$ photoelectrons were observed at ~458.8 eV and ~464.4 eV, indicating that elemental Ti was formed in the TiO_2 samples [12].

These results imply that Ti in all the TiO_2 samples exists as Ti (IV) after calcination at 500 °C. Based on the FESEM, TEM, XRD, and XPS results, although all the samples have the same crystal structures and chemical composition, morphologies ranging from nanoparticles to nanoflakes were formed. Therefore, a possible mechanism for a morphological change is explained in terms of the higher partial pressure of water [11] and the slower solidification of the charged jet [13], as the relative humidity increased. That is, for the case of the higher relative humidity, when a fluid jet erupted from the tip of the needle, the charged jet was formed to nanoflakes because of the higher partial pressure of water surrounding the jet resulting in

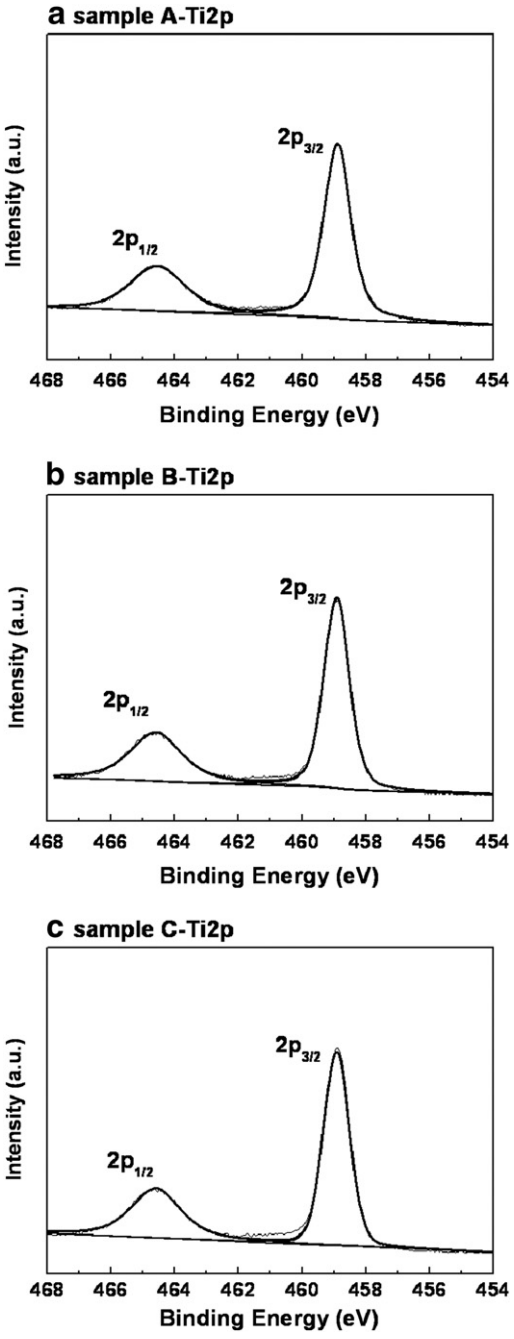

Fig. 4. XPS spectra of the Ti 2*p* core level for (a) sample A, (b) sample B, and (c) sample C.

the higher relative humidity. Also, the slower solidification process can allow the elongation of the charged jet due to the diminished evaporation rate of the jet, resulting in the formation of longer and thinner anatase-TiO_2 nanoflakes. Overall, anatase-TiO_2 nanoparticles can be successfully converted to anatase-TiO_2 nanoflakes via electrospray.

4. Summary

A change in morphology from anatase-TiO_2 nanoparticles to anatase-TiO_2 nanoflakes was induced by the electrospray process together with control of the relative humidity in the closed electrospray chamber, and these changes were demonstrated based on structural and chemical analyses of the samples by FESEM, TEM, XRD, and XPS. Although all samples formed had the same crystal structures and chemical composition, morphologies ranging from nanoparticles to nanoflakes could be synthesized by controlling the relative humidity during the electrospray process.

Acknowledgment

This work was supported by Grant No. 10031768 from the Ministry of Knowledge Economy (MKE) and the Fundamental R&D Program for Core Technology of Materials funded by the Ministry of Knowledge Economy, Republic of Korea.

References

[1] Ahn HJ, Choi HC, Park KW, Kim SB, Sung YE. J Phys Chem B 2004;108:9815–20.
[2] Choi HC, Ahn HJ, Jung YM, Lee MK, Shin HJ, Kim SB, et al. Appl Spectrosc 2004;58:598–602.
[3] Chen JS, Lou XW. Electrochem Commun 2009;11:2332–5.
[4] Feng X, Shankar K, Varghese OK, Paulose M, Latempa TJ, Grimes CA. Nano Lett 2008;11:3781–6.
[5] Tian ZR, Voigt JA, Liu J, Mckenzie B, Xu H. J Am Chem Soc 2003;125:12384–5.
[6] Wang G, Liu ZY, Wu JN, Lu Q. Mater Lett 2012;71:120–2.
[7] Modesto-Lopez LB, Biswas P. J Aerosol Sci 2010;41:790–804.
[8] Hwang D, Lee H, Jang SY, Jo SM, Kim D, Seo Y, et al. ACS Appl Mater Interfaces 2011;3:2719–25.
[9] Rezvanpour A, Wang CH. Chem Eng Sci 2011;66:3836–49.
[10] An GH, Jeong SY, Seong TY, Ahn HY. Mater Lett 2011;65:2377–80.
[11] Vrieze SD, Camp TV, Nelvig A, Hagstrom, Westroek P, Clerck KD. J Mater Sci 2009;44:1357–62.
[12] Moulder JF, Stickle WF, Sobol PE, Bomben KD. Handbook of X-ray photoelectron spectroscopy, physical electronics. Eden Pairie: Physical Electronics, Inc; 1995. p. 72–3.
[13] Tripatanasuwan S, Zhong Z, Reneker DH. Polymer 2007;48:5742–6.